Theoretical and Experimental Studies of SMES Configurations for Design Optimization

Jaime Gómez, Belén Pérez, Pilar Suárez, Alfredo Álvarez, and Belén Rivera

***Abstract*—In the current energy scenario, due to the increment in power generation from renewable sources, the importance of electrical storage systems has increased significantly, and as a consequence, the study of the improvement of its efficiency and the design of new storage systems also increased. Superconducting material permits the design of Superconducting Magnetic Energy Storage (SMES). The main problem of SMEs is the low energy density they have, what make the optimization of design to be one of the keys for inclusion of this elements in the power grid and other specific applications as, for instance, flux pumps. As the only basic forms for SMES, and with the objective of its mathematical optimization, this work (i) evaluates the mathematical equations for a real solenoidal winding, and (ii) develops the equivalent equations for a toroidal winding, from the electromagnetic laws. Then, (iii) a practical structure formed by short solenoids connected in series along a circular axis (quasi-toroidal structure) is studied. Due to the large number of equations involved in this case, the finite-element method in used here. Finally (iv), in order to validate the results without building the complete solenoid (impossible at the time), one of the magnetic coupling between two solenoids in the quasi-toroidal winding was developed according with the theoretical method, and experimentally tested. The study was carried out by programming different dimensions in order to make conclusions for a further development of an optimization algorithm. These conclusions are presented. This work is the first stage for the optimized design of a SMES, and presents the complete equations of the real toroidal winding as the base of the outline dimensions of a practical quasi-toroidal SMES.**

***Index Terms*—Efficiency, electrical storage systems, energy density, finite-element models, optimization of design, SMES, solenoids.**

I. Introduction

THE energy scene in the world is in a critical spot, fossil fuels, the main source of energy in many countries, are running out. Renewable energy sources are supposed to fill that role in the upcoming future, but they need energy storage systems in order to succeed. There are quite a lot of different technologies available when it comes to storing energy [1], [2], as illustrated in Figs. 1 and 2. SMES play a key role in that scene, presenting some elements that other technologies cannot provide, as efficiency [3] or response velocity [4], but, on the other hand, the weakness of this technology is the low energy density that it exhibits [5]. For this reason, when a SMES is calculated, a good design is especially necessary, and many authors have reported interesting solutions [6]–[9]. The optimization of dimensions, having into account an adequate constraint of parameters, helps to improve such a design. There are some interesting computer tools for optimization (MS Excel or Matlab, for instance, have specific tools for this task) but, in all of cases, the mathematic formulation of the problem is the key of the successful. In the follow section we develop the equations for the two main real configurations used for SMES design (solenoidal and toroidal configuration), which have been compared before [10] under different points of view. Starting from the outline dimensions obtained from the theoretical equations, a *fem* (finite elements method) model for a "quasi-toroidal" configuration, made from short solenoidal elements, is developed highlighting the parameters which must be used in a finer optimization of SMES.

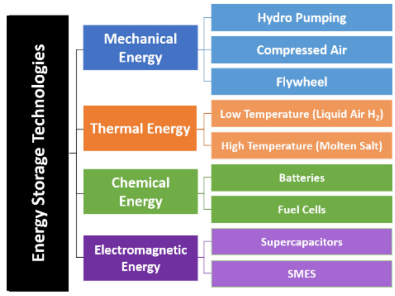

Fig. 1. Energy storage systems classification.

		Efficency (%)	Energy Density(kWh/m^3)	Capacity	Response Time
Hydro Pumping		65-85	1-2	100MWh-10GWh	sec-min
Compressed Air		60-70	2-6	10MWh-1GWh	sec-min
Flywheel		90	20-80	1kWh-100kWh	instant
Molten Salt		30	-	1MWh	sec-min
Liquid Air		60-70	-	15MWh-1GWh	sec
Batteries	NiCd	70-90	10-100	5kWh-10MWh	milisecond
	Pb-ácido	75-90	50-90		
	Li-ión	87-94	200-500		
	NaS	75	150-300		
Supercapacitors		90-94	10-30	-	milisecond
SMES		95	1-7	<20MWh	instant

Fig. 2. Comparison energy storage systems.

II. Theoretical Frame

The magnetic energy stored in a coil, with self-inductance L, supplied by a current I, is given by the following expression:

$$W = \frac{1}{2} LI^2 \tag{1}$$

Manuscript received November 26, 2020; revised January 14, 2021; accepted February 2, 2021. Date of publication February 16, 2021; date of current version April 2, 2021. This work was supported in part by the Government of Extremadura through the funding GR18092, IB18076 and in part by FEDER. *(Fondo Europeo de Desarrollo Regional). (Corresponding author: Belén Pérez.)*

The authors are with the Department of Electrical Engineering, and Electrical Applications of Superconductors (EAS) Group of the University of Extremadura, 06006 Badajoz, Spain (e-mail: belenpc@unex.es).

Color versions of one or more figures in this article are available at https://doi.org/10.1109/TASC.2021.3059609.

Digital Object Identifier 10.1109/TASC.2021.3059609

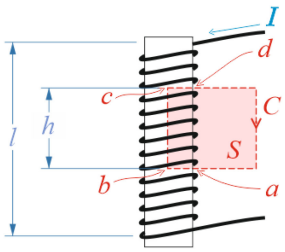

Fig. 3. Ideal solenoid parameters for magnetic flux density integration.

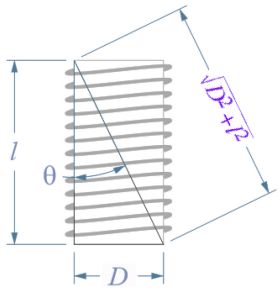

Fig. 4. Real solenoid. Reference triangle for the calculation of κ.

The inductance of a coil is defined as the variation of its own magnetic flux, Φ, with its current. Taking N as the number of turns in the coil, the result for the inductance is:

$$L = N\frac{d\Phi}{dI} = N\frac{d}{dI}\left(\vec{B}\cdot\vec{A}\right), \tag{2}$$

where $\vec{A}$ is the surface vector of the normal section of the coil. When $\vec{A}$ is parallel to $\vec{B}$, (2) can be written as following:

$$L = N\frac{d}{dI}(BA) \tag{3}$$

Thus, in order to calculate the magnetic energy stored in a coil, it is necessary to determine the expression of the magnetic field and then the inductance.

We present here the more common configuration to build a real SMES, i.e., the solenoidal and toroidal configurations

A. Real Solenoid

The magnetic field created by a current I in a solenoid with radius r and length l is well known when $l >> r$, and its N turns are really close to each other (ideal solenoid). Fig. 3 shows a scheme of this solenoid. In order to integrate the Ampere's law, a close path C like in Fig. 3 is chosen.

The magnetic flux density vector $\vec{B}$ inside the solenoid is supposed to be constant in all the points:

$$\vec{B} = \frac{\mu_0 IN}{l}\,\vec{k} \tag{4}$$

($\vec{k}$ is the axial unit vector).

Using (4) in (3), the inductance can be written:

$$L = N\frac{dBA}{dI} = \frac{\mu_0 N^2\pi r^2}{l}. \tag{5}$$

In real cases, the obtained result (5) is valuable only in the central region of long solenoids, in which the magnetic field is parallel, and the border effects are negligible. Near the solenoid ends (5) is no longer valid, and its calculus becomes excessively complex. For this reason, in order to fit the ideal result to the real value, correction parameters are generally used in engineering. The most widely correction used was developed by the Japanese Physicist Hantaro Nagaoka [11]. According to Nagaoka, the inductance of a short solenoid like that in Fig. 4, can be expressed as following:

$$L = \frac{\mu_0 N^2\pi r^2}{l}\,K_L, \tag{6}$$

where the correction factor K_L $(0 < K_L < 1)$, is known as Nagaoka coefficient, and has the following form:

$$K_L = \frac{8r}{3l\pi}\left[\frac{2\kappa^2-1}{\kappa^3}E(\kappa) + \frac{1-\kappa^2}{\kappa^3}K(\kappa) - 1\right]. \tag{7}$$

In (7) $E(\kappa)$ and $K(\kappa)$, are elliptic integrals of first and second kind respectively, being κ the module of the integrals, a parameter that depends on the dimensions of the solenoid, and is given by:

$$\kappa = \sin\theta = \frac{D}{\sqrt{D^2+l^2}}. \tag{8}$$

where $D = 2r$ is the diameter of the solenoid cross section, as Fig. 4 shows.

Substituting (7) in (6) and the result in (1) we get the energy stored in the real solenoid:

$$W = \frac{\mu_0 N^2 I^2 D^3}{3l^2}\left[\frac{2\kappa^2-1}{\kappa^3}E(\kappa) + \frac{1-\kappa^2}{\kappa^3}K(\kappa) - 1\right] \tag{9}$$

This is the equation, with the adequate constrictions (e.g., minimum volume to improve the energy density) that have to be used in a mathematical optimization of the design as above mentioned.

Nagaoka approach is often used in the study of solenoidal SMES (see e.g., [6] or [9]), but no an equivalent equation is found for a toroidal geometry. In the next section we present the study of such an equation.

B. Real Toroid

As in the case of the solenoid, the magnetic flux density in an N turns ideal toroid with main radius R, cross section radius $r << R$, and current I, is easy to evaluate by application of Ampere's law in cylindrical coordinates:

$$\vec{B} = \frac{\mu_0 IN}{2\pi R}\,\vec{\varphi} \tag{10}$$

($\vec{\varphi}$ is the angular unit vector).

In the ideal toroid, (10) is valid for all the points of the cross section. If this does not happen, the magnetic field $\vec{B}$ on each point depends on the length of the field line used to integrate the Ampere's law. Fig. 5 helps to understand this. The magnetic field in a point separated by R' from the center of the toroid, is:

$$\vec{B}\,(R') = \frac{\mu_0 IN}{2\pi R'}\,\vec{\varphi}\,(R-r < R' < R+r). \tag{11}$$

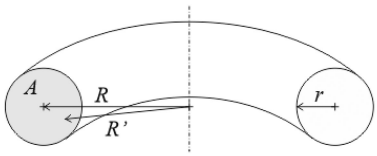

Fig. 5. Toroidal parameters for calculus.

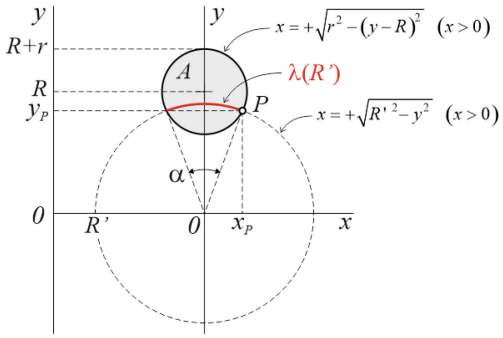

Fig. 6. Non-ideal torus cross section.

The magnetic flux, Φ, can be calculated with the aid of Fig. 6. There, $\lambda(R')$ represents an arc with radius R' inside the cross section A of the toroid. $\vec{B}$ is constant in $\lambda(R')$ and parallel to vector $\vec{A}$, so we can integrate the magnetic flux as following:

$$\Phi = \int_{\mathrm{A}} \mathrm{B}\,(\mathrm{R}')\,\mathrm{dA} = \int_{\mathrm{A}} \mathrm{B}\,(\mathrm{R}')\,\lambda(\mathrm{R}')\mathrm{dR}'. \tag{12}$$

In order to determinate $\lambda(R')$, the angle α that sustains it (see Fig. 6) must be determined. To do that, the coordinates (x_P, y_P) of the point *P* have to be obtained. This point is the intersection, for x > 0, of the circumferences in Fig. 6, the equations of which appear next to them. Equaling these equations and taking just positive values of x, the following result is obtained:

$$y_P\ (R') = \frac{R'^2 + R^2 - r^2}{2R},$$
$$x_P\ (R') = \sqrt{R'^2 - y_p^2} \tag{13}$$

From these results, the angle α can be calculated as:

$$\alpha\ (R') = 2\ \arctan\frac{x_P}{y_P} = 2\arctan\left(\frac{2RR'^2}{R'^2 + R^2 - r^2} - 1\right)^{\frac{1}{2}} \tag{14}$$

and, therefore,

$$\lambda\ (R') = R'\ \alpha\ (R') = 2R'\arctan\left(\frac{2RR'^2}{R'^2 + R^2 - r^2} - 1\right)^{\frac{1}{2}} \tag{15}$$

The flux can be found replacing (11) and (15) in (12):

$$\Phi = \mu_0\, IN \int_{R-r}^{R+r} actan\left(\frac{2RR'^2}{R'^2 + R^2 - r^2} - 1\right)^{\frac{1}{2}} dR' \tag{16}$$

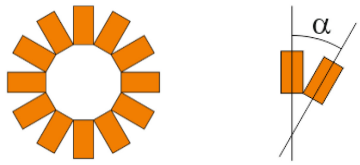

Fig. 7. Scheme of a modular toroid made up of short solenoids.

Finally, using (16) in (2) and the result in (1), the equation of the energy in a real toroidal coil is found out:

$$W = \frac{1}{2}\mu_0\, N^2 I^2 \int_{R-r}^{R+r} \arctan\left(\frac{2RR'^2}{R'^2 + R^2 - r^2} - 1\right)^{\frac{1}{2}} dR' \tag{17}$$

As in the solenoidal coil, this is the equation to be used in a mathematical optimization of a toroidal SMES.

III. Quasi-Toroidal Structure

From a practical point of view, the toroidal configuration is the most convenient form for a SMES. However, manufacturing issues and structural requirements recommend using a modular quasi-toroidal structure forms by short straight solenoids [12]. Fig. 7 approximates the shape of this structure.

As can be noted, the angle between elements determines the number of them, and the aspect ratio of the toroid determines the aspect ratio of the element.

For optimization of this configuration, a first study of the complete real solenoid as in Section II must be done. After taking a decision of the toroid main radius and cross-section radius, the effect of the modular construction must be studied. Nevertheless, the theoretical formulation of an *N*-coils modular toroid involves *N!* equations corresponding to all *N!* possible couplings between pairs of coils.

The computer resources recommend addressing this study by modeling the system and experimentally validating the model. Here we present an approach to this study.

A. Modelling the Modular Toroid

Using Comsol Multiphysics software, the model of a modular toroid was programed to be studied by the finite element method (*fem*). Because no specific superconducting properties are involved in this stage, we have used the Electromagnetic Fields module (Physic). This Physic uses the Maxwell equations to solve the vector potential. The possibility of defining variable and calculable parameters in the model permits easily to compare results.

To illustrate the proceeding, two modular toroids, with the same coils but different angle between them, were simulated. The parameters are listed in Table I.

Fig. 8 shows the graphical results for the magnetic field and Table II the results for the energy with different currents.

B. Testing the Model for a Single Coupling

Due to the impossibility of building a real superconducting modular toroidal coil to compare with the simulation results, a third system was studied. The objective is to validate the model (initial and boundary conditions, mainly) using it with

TABLE I
PARAMETERS OF TWO MODULAR TOROIDAL SMES TO BE COMPARED

N_{COIL}	420	420	Turns per coil
r_{Ext} (mm)	33,50	33,50	Coil external radius
r_{Int} (mm)	10,00	10,00	Coil internal radius
a (mm)	29,50	29,50	Coil width
alfa (°)	15	30	angle between coils
R_{Int} (mm)	113,96	51,53	Toroid external radius
R_{med} (mm)	148,50	87,00	Toroid internal radius

(∗) Angle is the only programed difference between models. The toroids radii below are calculated as a function of this by the model.

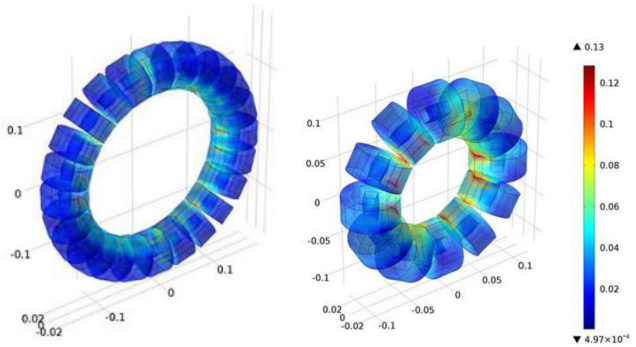

Fig. 8. Magnetic flux density (T) of the modular toroid for a current of 7 A. (a) 15° angle between coils and (b) 30° angle between coils.

TABLE II
MAGNETIC ENERGY STORED IN THE MODULAR TOROID AT 15° AND 30°

15° Torus		30° Torus	
I (A)	W_{torus} (J)	I (A)	W_{torus} (J)
1,2	8,4E-02	1,2	4,2E-02
2,9	4,8E-01	2,8	2,5E-01
4,6	1,2E+00	4,6	6,8E-01
6,9	2,8E+00	7,0	1,6E+00
120,0	7,3E+02	120,0	4,6E+02

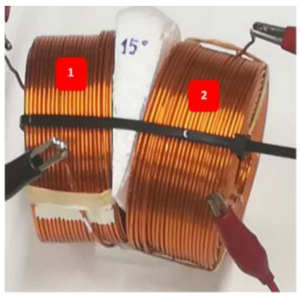

Fig. 9. Detail of the coupling tested for an angle of 15° between coils.

a simplified system that presents a geometry feasible to build. This system (Fig. 9) consist of two individual coils separated by the same two angles used before.

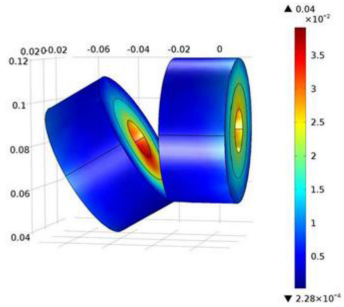

Fig. 10. Magnetic flux density (T) for the 30° coupling with 2.8 A.

TABLE III
ENERGIES STORED IN TWO COILS COUPLING AT 15° AND 30°

Coils at 15°		Coils at 30°	
I (A)	W (J)	I (A)	W (J)
1.2	0.0079	1.2	0.0075
2.9	0.0461	2.8	0.0408
4.6	0.1160	4.6	0.1101
6.9	0.2609	7.0	0.2548

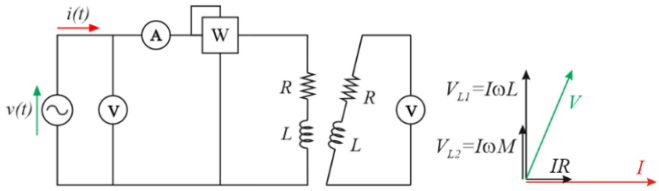

Fig. 11. Electrical circuit and sinusoidal steady state vector diagram corresponding to the experimental setup.

The model previously used was adapted for this case and the computational results were obtained. As an example, Fig. 10 shows the magnetic field in the 30° coupling with 2.8 A.

The energies stored in both configurations, for different currents, are reported in Table III.

As an experimental test to verify the validity of this results, the setup in Fig. 11 was used. This is the conventional no-load test for couplings or transformers whose vector diagram in sinusoidal steady state (*sss*) is shown there too.

As can be reviewed in literature (see, e.g., [13]), by measuring in *sss* the real power P, and the effective (rms) values of the current I and the source voltages V, the value of R (in primary) can be calculated and then, L and M –note that the voltage in the secondary voltmeter is V_{L2}, as this side is under no-load conditions during the test. The energy in the couple of identical coils carrying the same current is calculated as:

$$W = LI^2 + MI^2. \tag{18}$$

All the measurements and calculus programmed in the spreadsheet are summarized in Table IV.

Finally, Table V compares the energies obtained in the simulation with those experimentally calculated. The relative error of the measurements has also been included in the table. As can be seen, the experimental results fit satisfactorily the model results, which gives validity to it and, therefore, to the model of the complete superconducting quasi-toroidal SMES.

TABLE IV
MEASUREMENTS AND RESULTS OBTAINED FROM THE EXPERIMENTAL TESTS

Measurements for coils at 15°				Results					
V (V)	I (A)	P (W)	V_{L2} (V)	R (Ω)	V_R (V)	V_{L1} (V)	L (H)	M (H)	**W (J)**
2.1	1.20	1.3	0.34	0.903	1.1	1.8	0.004772	0.000902	**0.0082**
5.0	2.85	7.4	0.82	0.911	2.6	4.3	0.004772	0.000916	**0.0462**
8.2	4.70	19.8	1.31	0.896	4.2	7.0	0.004765	0.000887	**0.1248**
12.4	6.93	45.7	1.99	0.952	6.6	10.5	0.004823	0.000914	**0.2755**
Measurements for coils at 30°				**Results**					
V (V)	I (A)	P (W)	V_{L2} (V)	R (Ω)	V_R (V)	V_{L1} (V)	L (H)	M (H)	**W (J)**
2.1	1.15	1.2	0.25	0.907	1.0	1.8	0.005044	0.000692	**0.0076**
4.9	2.80	7.1	0.61	0.906	2.5	4.2	0.004767	0.000693	**0.0428**
8.1	4.60	19.4	1.01	0.917	4.2	6.9	0.004785	0.000699	**0.1160**
12.3	7.00	45.3	1.53	0.924	6.5	10.5	0.004756	0.000696	**0.2672**

TABLE V
COMPARISON BETWEEN THE SIMULATION AND EXPERIMENTAL RESULTS

Coils at 15°				Coils at 30°			
I(A)	Simulation	Experimental	ε_r (%)	I(A)	Simulation	Experimental	ε_r (%)
1.2	0.0079	0.0082	3.42	1.2	0.0075	0.0076	1.30
2.9	0.0461	0.0462	0.22	2.8	0.0408	0.0428	4.99
4.6	0.1160	0.1248	7.63	4.6	0.1101	0.1160	5.45
6.9	0.2609	0.2755	5.61	7.0	0.2548	0.2672	4.83

IV. CONCLUSION

A mathematical model of the energy in a real toroidal coil have been developed following the methodology used by Nagaoka [11] for the real solenoidal coil.

The formulation contains all the elements necessary for the SMES optimization by means of the available tools, and with the adequate constrictions.

For the practical quasi-toroidal coil made from short solenoidal coils, a model built using Comsol Multiphysics software is a simple but effective tool to substitute the high number of equations involved in the theoretical analysis.

The model has been experimentally tested with satisfactory results.

REFERENCES

[1] A. Evans, V. Strezov, and T. J. Evans, "Assessment of utility energy storage options for increased renewable energy penetration," *Renewable Sustain. Energy Rev.*, vol. 16, 2012. [Online]. Available: https://doi.org/10.1016/j.rser.2012.03.048

[2] S. Koohi-Fayegh and M. A. Rosen, "A review of energy storage types, applications and recent developments," *J. Energy Storage*, vol. 27, 2020. [Online]. Available: https://doi.org/10.1016/j.est.2019.101047

[3] R. Holla, "Energy storage methods - Superconducting magnetic energy storage - A Review," *J. Undergraduate Res.*, vol. 5-1, 2015. [Online]. Available: https://doi.org/10.5210/jur.v8i1.7540

[4] A. K. Rohit *et al.*, "An overview of energy storage and its importance in indian renewable energy sector: Part I—Technologies and comparison," *J. Energy Storage*, vol. 13, 2017. [Online]. Available: https://doi.org/10.1016/j.est.2017.06.005

[5] D. O. Akinyele and R. K. Rayudu. "Review of energy storage technologies for sustainable power networks," *Sustain. Energy Technol. Assessments*, vol. 8, 2014. [Online]. Available: https://doi.org/10.1016/j.seta.2014.07.004

[6] P. R. Raut, H. J. Bahirat, and M. D. Atrey, "Analytical approach for optimal HTS solenoid design," *IEEE Trans. Appl. Supercond.,* vol. 31, no. 2, Mar. 2021, Art. no. 4900209.

[7] A. W. Zimmermann and S. M. Sharkh, "Design of a 1 MJ/100 kW high temperature superconducting magnet for energy storage," *Energy Rep.*, vol. 6, 2020. [Online]. Available: https://doi.org/10.1016/j.egyr.2020.03.023

[8] S. Noguchi, Y. Inaba, and H. Igarashi, "An optimal configuration design method for HTS-SMES coils taking account of thermal and electromagnetic characteristics," *IEEE Trans. Appl. Supercond.*, vol. 18, no. 2, pp. 762–765, Jun. 2008.

[9] N. Sugimoto *et al.*, "Compact SMES with a superconducting film in a spiral groove on a Si wafer formed by MEMS technology with possible high-energy storage volume density comparable to that of rechargeable batteries," *Supercond. Sci. Technol.*, vol. 30, 2017. [Online]. Available: https://doi.org/10.1088/0953-2048/30/1/015014

[10] A. Morandi, M. Fabbri, B. Gholizad, F. Grilli, F. Sirois, and V. M. R. Zermeño, "Design and comparison of a 1-MW/5-s HTS SMES with toroidal and solenoidal geometry," *IEEE Trans. Appl. Supercond.*, vol. 26, no. 4, Jun. 2016, Art. no. 5700606.

[11] H. Nagaoka, "The inductance coefficients of solenoids," *J. College Sci.*, vol. 27, pp. 18–33, 1909.

[12] A. Hekmati and R. Hekmati, "Double pancake superconducting coil design for maximum magnetic energy storage in small scale SMES systems," *Cryogenics*, vol. 80-1, 2016. [Online]. Available: https://doi.org/10.1016/j.cryogenics.2016.09.009

[13] S. Nasar, "Electric machines and electromechanics," in *Schaum's Outline Series*. Mcgraw-HILL. 2nd ed. 1997.